View Online / Journal Homepage / Table of Contents for this issue
Dynamic Article Links

Journal of Materials Chemistry

Cite this: J. Mater. Chem., 2012, 22, 14119

www.rsc.org/materials

PAPER

BODIPY-based conjugated polymers for broadband light sensing and harvesting applications†

Diego Cortizo-Lacalle,[a] Calvyn T. Howells,[b] Salvatore Gambino,[b] Filipe Vilela,[a] Zuzana Vobecka,[a] Neil J. Findlay,[a] Anto R. Inigo,[a] Stuart A. J. Thomson,[b] Peter J. Skabara*[a] and Ifor D. W. Samuel*[b]

Received 17th April 2012, Accepted 2nd June 2012
DOI: 10.1039/c2jm32374e

Published on 18 June 2012 on http://pubs.rsc.org | doi:10.1039/C2JM32374E
Downloaded by University of Strathclyde on 23 August 2012

The synthesis of novel low band-gap polymers has significantly improved light sensing and harvesting in polymer–fullerene devices. Here the synthesis of two low band-gap polymers based on the 4,4-difluoro-4-bora-3*a*,4*a*-diaza-*s*-indacene core (BODIPY), and either bis(3,4-ethylenedioxythiophene) (bis-EDOT) or its all-sulfur analogue bis(3,4-ethylenedithiathiophene) (bis-EDTT) are described. The polymers demonstrate ambipolar charge transport and are shown to be suitable for broadband light sensing and solar energy harvesting in solution-processable polymer–fullerene devices.

Introduction

Since the fabrication of the first organic photovoltaic (OPV) cell in 1986,[1] OPVs have attracted considerable interest.[2] The possibility of fabricating flexible, low-cost, light-weight devices from solution, with materials that have a readily tuneable band-gap, makes them attractive. In 1995, the bulk heterojunction (BHJ) structure was devised, revolutionising OPVs.[3,4] BHJ-OPVs consist of an interpenetrating network of a donor and an acceptor material. One promising combination is a blend of a conjugated polymer and a soluble fullerene derivative. Polymer–fullerene devices have demonstrated power conversion efficiencies (PCE) greater than 7%[5,6] and the ultrafast electron transfer from polymer to fullerene in BHJ allows for polymer–fullerene devices to be used as photodetectors for light sensing applications.[7] The fine network in polymer–fullerene BHJs forms small domains of both components, allowing excitons formed within the active layer to diffuse to the donor–acceptor interface within the exciton diffusion length.[8,9,10] The most studied of all polymer–fullerene blends is that of poly(3-hexylthiophene) (P3HT) and [6,6]-phenyl-C_{61}-butyric acid methyl ester (PCBM), which favours effective charge transfer from the lowest unoccupied molecular orbital (LUMO) of the photoexcited polymer to the LUMO of the acceptor. P3HT:PCBM blends can have PCEs of up to 5%.[11] The main drawback of P3HT is its band-gap of ~1.9 eV.[12] In order to overcome poor photon harvesting and increase absorption, new low band-gap polymers are required.

One approach for obtaining low band-gap polymers is based on alternating donor–acceptor units along the polymer backbone, forming partial charge separation between each moiety. This approach increases the highest occupied molecular orbital (HOMO) level and at the same time decreases the LUMO level, giving a lower band-gap material and red-shifting the absorption spectrum of the polymer. These low band-gap polymers are usually synthesised by cross-coupling reactions of the donor and acceptor units. Different donors such as thiophene derivatives, fused thiophenes, fluorene, carbazole, silafluorene, cyclopentadithiophene and their derivatives have been widely used.[13] Amongst acceptor units, benzothiadiazole,[14] thienopyrazine,[15] and diketopyrrolopyrrole[16] are the most widely used. Though important, the low band-gap nature of donor polymers is not the only requirement to obtain high PCEs, as a multifactorial approach is necessary. The relative positions of the HOMO–LUMO levels of both polymer and acceptor have to be controlled in order to maximise the open circuit voltage (V_{oc}). However, an energy offset of >0.3 eV between the LUMOs of the donor and acceptor is required for exciton dissociation.[17] Besides having a low band-gap, there are other aspects that impact device performance such as mobility, morphology and solubility, making the search for new OPV materials challenging.

The BODIPY 4,4-difluoro-4-bora-3*a*,4*a*-diaza-*s*-indacene core (Fig. 1) has attracted much attention during the last 20 years due to its strong absorption–emission and fluorescence properties, as well as chemical robustness.[18] BODIPY derivatives have been used for different applications such as biological tags with visible/near IR emission, mechanical rotors, lasing, dye-sensitized solar cells, electroluminescence and electrogenerated chemiluminescence.[19] In addition to their electronic properties, BODIPY derivatives also exhibit variable redox chemistry, and they have been used as electron donors and acceptors.[20,21] We have recently published the electrochemical synthesis of a redox stable, low band-gap polymer based on an EDOT–BODIPY–EDOT

[a]*WestCHEM, Department of Pure and Applied Chemistry, University of Strathclyde, Glasgow, G1 1XL, UK. E-mail: peter.skabara@strath.ac.uk*
[b]*Organic Semiconductor Centre, SUPA, School of Physics and Astronomy, University of St Andrews, St Andrews, KY16 9SS, UK. E-mail: idws@st-and.ac.uk*

† Electronic supplementary information (ESI) available. See DOI: 10.1039/c2jm32374e

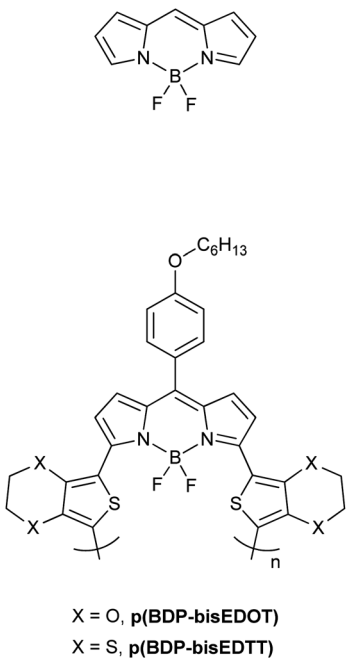

Fig. 1 Structures of the BODIPY core (top) and target polymers.

unit.[22] Whereas other BODIPY based polymers have been electrochemically synthesised, mainly through the *beta*-positions of the pyrrole rings,[23] we have focused on polymerization through the *alpha*-positions.

In this paper the synthesis of two novel low band-gap polymers bearing a BODIPY core as an electron acceptor and either a bis-EDOT or bis-EDTT (the all-sulfur analogue), as an electron donor is described. The polymer with the largest short circuit current density (J_{sc}) was selected for time of flight (TOF) measurements. These measurements show **p(BDP-bisEDOT)** to have electron and hole mobilities of the same order of magnitude, implying ambipolar charge transport. Polymer-only devices had a power conversion efficiency of 0.06% and 0.13% for **p(BDP-bisEDTT)** and **p(BDP-bisEDOT)**, respectively. Polymer–fullerene devices demonstrated power conversion efficiencies of 0.45% and 0.95% for **p(BDP-bisEDTT)** and **p(BDP-bisEDOT)**, respectively. These devices demonstrate a broad spectral response, making these materials possible candidates for future broadband organic photodiodes and photovoltaics.

Experimental

^{1}H and ^{13}C NMR spectra were recorded, unless stated otherwise, at room temperature on a Bruker DRX500 at 500 and 125 MHz or a Bruker Avance 400 instrument at 400 and 100 MHz; chemical shifts are given in ppm and all *J* values are in Hz. Mass spectra (ES) were recorded on a Thermo Finnigan LCQDuo system using direct infusion. MALDI-TOF (AXIMA-CRF) mass spectra were recorded on a Kratos spectrometer. Column chromatography was carried out on silica gel Zeoprep 60 Hyd (40–63 μm mesh). Alfa Aesar supplied the filter aid celite hyflo-super-cel (dioxosilane) used for purification. Solvents were removed using a rotary evaporator (vacuum supplied by low vacuum pump) and, where necessary, a high vacuum pump was used to remove residual solvent. All distillations were performed on a Kugelrohr Z24 with high vacuum pump. Dry solvents were collected through a purification system. Unless stated otherwise, all reagents used were obtained commercially from Sigma Aldrich or Alfa Aesar and used without any purification.

Device fabrication

Solar cells were prepared on indium tin oxide (ITO) coated glass substrates, purchased from Xin Yan Technology Ltd (15 Ω per □). The substrates were masked and etched in hydrochloric acid (37%) for 20 min defining a 4 mm wide bottom contact and subsequently cleaned in an ultrasonic bath with deionised water, acetone and isopropanol successively for 15 min. The substrates were then dried with a nitrogen gun before being placed in an oxygen plasma asher for 5 min. Poly(3,4-ethylenedioxythiophene):poly(styrenesulfonate) (PEDOT:PSS) from H. C. Starck (Baytron AI4083) was spin-coated on top of the ITO at 4000 rpm and dried on a hot plate at 120 °C for 20 min. For active layer deposition, substrates were placed in a nitrogen-filled glovebox. Neat devices were prepared from a 15 mg ml^{-1} solution. Bulk films containing various donor/acceptor ratios were spin-coated from a 20 mg ml^{-1} solution. A few drops of carbon disulfide were added to each chlorobenzene solution before spin coating for enhanced solubility. [6,6]-Phenyl-C_{71}-butyric acid methyl ester (C_{70}-PCBM) from Solenne B.V. company was used as the acceptor in BHJ. Spin coating BHJ at 1000 rpm produced films of ~110 nm thickness. Active layer thicknesses were measured using a Dektak 150 M stylus profilometer. Devices were placed into a vacuum chamber for aluminium deposition. 1.4 mm wide and 200 nm thick aluminium electrodes were thermally evaporated at a pressure of 1.8×10^{-6} mbar and a deposition rate of 0.4 nm s^{-1} producing devices with an active area of 0.06 cm^2. After back electrode deposition, devices were annealed for 20 min at 120 °C. Immediately after annealing, devices were encapsulated with a glass cover slip using a UV activated optical adhesive from Thorlabs. Devices were removed from the glove box and characterised, in air, using a K. H. Steuernagel AM 1.5G solar simulator and a Keithley 2400 source-measure unit. Light intensities were verified with a calibrated thermopile from coherent model number LM-1. IPCE spectra were measured using a NPL calibrated photodiode, Bentham TMc300 monochromator and a Keithley 6517A picoammeter.

For TOF measurements a 10 mg ml^{-1} chlorobenzene solution was prepared and drop-cast onto plasma ashed ITO substrates, resulting in 1.1 μm thick films. The samples were placed in an evaporator where, under high vacuum, a semitransparent (30 nm) aluminium layer was deposited through a shadow mask. The device was then placed in a cryostat where photogeneration of charge carriers was achieved by exciting the BODIPY with a 580 nm pulsed dye laser. For electron mobility measurements the sample was illuminated through the negatively biased ITO contact and the electrons were collected at the Al contact, whilst for hole mobility measurements the sample was illuminated through the positively biased Al contact and holes were collected at the ITO contact. In both cases the resulting photocurrent was passed through a variable sensing resistor and recorded on a digital storage oscilloscope. The carrier mobility was determined from the transit time (t_{tr}) using the following equation:

Published on 18 June 2012 on http://pubs.rsc.org | doi:10.1039/C2JM32374E
Downloaded by University of Strathclyde on 23 August 2012

 This journal is © The Royal Society of Chemistry 2012

$$\mu = \frac{L^2}{V \times t_{tr}}$$

where L is the thickness of the organic layer and V is the external applied voltage.

5-(4-*n*-Hexyloxyphenyl)dipyrromethane (2)

Freshly distilled pyrrole (50 ml, 0.727 mol) and 4-hexyloxy benzaldehyde **1** (5 g, 24.2 mmol) were added to a 250 ml round bottom flask, the mixture was purged with N_2 for 10 minutes and trifluoracetic acid (0.03 ml) was added. The mixture was stirred for 1 h at room temperature until all the benzaldehyde had been consumed (followed by TLC). The reaction mixture was washed with a solution of Na_2CO_3, extracted with CH_2Cl_2, dried over $MgSO_4$, filtered and evaporated. The crude product was purified by Kugelrohr vacuum distillation at 200 °C, 6.6×10^{-3} mbar, to give 5.7 g (73%) of a yellow oil. Elemental analysis requires: $C_{21}H_{26}N_2O$, C, 78.22; H, 8.13; N, 8.69; found: C, 77.75; H, 8.13; N, 9.17%; MS GC/EI; 322.06; ^{1}H NMR ($CDCl_3$) 7.92 (2H, d, J = 8.9); 7.13 (2H, d, J = 8.8), 6.86 (2H, d, J = 8.4), 6.69 (2H, d, J = 4.5), 6.17 (2H, m), 5.93 (2H, m), 5.43 (1H, s), 3.95 (2H, t, J = 6.5), 1.79 (2H, m), 1.47 (2H, m), 1.35 (4H, m) and 0.92 (3H, m); ^{13}C NMR (100 MHz, $CDCl_3$) 158.2, 134.0, 133.0, 129.4, 117.2, 114.7, 108.5, 107.1, 68.1, 43.2, 31.7, 29.39, 25.87, 22.7, 14.1.

1,1-Dichloro-5-(4-*n*-hexyloxyphenyl)dipyrromethene (3)

Compound **2** (3.7 g, 11.5 mmol) was dissolved in dry THF (80 ml) and cooled to −78 °C under N_2. A suspension of NCS (3.14 g, 23.5 mmol) in dry THF (60 ml) was added and the reaction mixture was stirred at −78 °C for 1.5 h and then warmed to room temperature overnight. The mixture was washed with water (3 × 150 ml) and extracted with CH_2Cl_2 (3 × 200 ml). The organic layer was dried over Na_2SO_4, filtered and evaporated. The residue was dissolved in CH_2Cl_2 (200 ml), and DDQ (2.6 g, 12.5 mmol) was added and stirred at room temperature for 1.5 h. The solvent was evaporated and the crude product was purified by column chromatography (CH_2Cl_2/hexane – 3/7, R_f = 0.26) to give 1.7 g (38%) of a green solid. Elemental analysis requires: $C_{21}H_{22}Cl_2N_2O$, C, 64.79; H, 5.70; N, 7.20; found: C, 64.79; H, 5.98; N, 7.25%; MS GC/EI; 389.07; ^{1}H NMR ($CDCl_3$) 12.48 (1H, bs), 7.37 (2H, d, J = 8.6), 6.96 (2H, d, J = 8.6), 6.60 (2H, d, J = 4.2), 6.27 (2H, d, J = 4.2), 4.03 (2H, t, J = 6.5), 1.84 (2H, m), 1.51 (2H, t, J = 6.5), 1.38 (4H, m) and 0.93 (3H, m); ^{13}C NMR (100 MHz, $CDCl_3$) 160.5, 141.4, 140.2, 138.7, 132.5, 130.2, 127.7, 116.8, 113.9, 68.3, 31.7, 29.3, 25.8, 22.7, 14.1, m.p.: 78–80 °C.

3,5-Dichloro-8-(4-*n*-hexyloxyphenyl)-4,4-difluoro-4-bora-3*a*,4*a*-diaza-*s*-indacene (4)

A solution of **3** (1.0 g, 2.57 mmol) and Et_3N (3.6 ml, 25.7 mmol) in dry dichloromethane (100 ml) was stirred under nitrogen at room temperature for 10 min. Then $BF_3 \cdot Et_2O$ (4.9 ml, 38.5 mmol) was added slowly over 10 min. The resulting solution was stirred for 22 h, then washed with water (3 × 70 ml), dried over anhydrous Na_2SO_4, filtered and evaporated to dryness. The residue was loaded onto silica gel and purified by flash column chromatography, eluting with EtOAc/hexane (1/4), (R_f = 0.28), yielding 1.1 g, (95%) of a violet oil. Elemental analysis requires: $C_{21}H_{21}BCl_2F_2N_2O$, C, 57.70; H, 4.84; N, 6.41; found: C, 57.95; H, 4.49; N, 5.99%. MS MALDI TOF: 473 (hydrochloride salt); ^{1}H NMR ($CDCl_3$) 7.43 (2H, d, J = 8.8), 7.03 (2H, d, J = 8.7), 6.89 (2H, d, J = 4.28), 6.44 (2H, d, J = 4.4), 4.05 (2H, t, J = 6.5), 1.85 (m, 2H), 1.51 (2H, t, J = 6.5), 1.36 (4H, m), 0.94 (3H, t, J = 7.0); ^{13}C NMR ($CDCl_3$) 161.8, 144.2, 144.0, 133.6, 132.3, 131.4, 124.5, 118.5, 114.6, 68.4, 31.5, 29.1, 25.70, 22.60, 14.0.

7,7′-Bis(trimethylstannyl)-2,2′,3,3′-tetrahydro-5,5′-bithieno[3,4-*b*][1,4]dioxine (6)

Bis-EDOT **5** (1.13 g, 4 mmol) was dissolved in dry THF (50 ml) and cooled to −80 °C. *n*-Butyl-lithium (4 ml, 2.5 M in hexanes, 10.0 mmol) was carefully added and the reaction was stirred for 30 min. Trimethyltin chloride (12 ml, 1 M in hexane, 12 mmol) was added keeping the reaction at −60 °C. The reaction was slowly warmed to room temperature and left stirring under nitrogen overnight. The solvent was removed and the solid was dissolved in CH_2Cl_2 (50 ml), washed with water (3 × 50 ml), dried over Na_2SO_4, filtered and evaporated to dryness to obtain a brown solid. The solid was recrystallised from hexane to obtain 2.2 g of a beige solid (81%). ^{1}H NMR ($CDCl_3$) 4.33–4.30 (4H, m), 4.24–4.21 (4H, m) and 0.38 (18H, s).

2,2′,3,3′-Tetrahydro-5,5′-bithieno[3,4-*b*][1,4]dithiine (8)

To a solution of EDTT (**7**) (3.83 g, 22 mmol) in dry THF (125 ml) cooled to −80 °C, was slowly added *n*-butyl-lithium (14 ml of 1.6 M solution in THF, 1.05 eq., 23 mmol). When the reaction temperature reached 0 °C, the solution was stirred for an extra 2 h at this temperature, before adding $CuCl_2$ (3.1 g, 1.05 eq., 23 mmol) in one portion. The reaction mixture was stirred overnight at 0 °C. The solvent was then removed and the crude mixture was dissolved in CH_2Cl_2 (50 ml), washed with water (3 × 50 ml), dried over Na_2SO_4, filtered and evaporated to dryness. The resulting mixture was loaded onto silica gel and purified by flash column chromatography, eluting with EtOAc/hexane (1/3), to afford a yellow powder (1.9 g, 50%) that was used in the next stage without further purification. ^{1}H NMR ($CDCl_3$) 7.08 (2H, s) and 3.25 (8H, br s).

7,7′-Bis(trimethylstannyl)-2,2′,3,3′-tetrahydro-5,5′-bithieno[3,4-*b*][1,4]dithiine (9)

To a solution of bis-EDTT (330 mg, 0.95 mmol) in dry THF (100 ml) and cooled to −80 °C, was slowly added *n*-butyl-lithium (1 ml of 2.5 M solution in hexane, 2.5 mmol). The reaction was stirred under nitrogen till the temperature reached −50 °C, before being cooled down again to −80 °C and Me_3SnCl (4 ml, 1 M in hexane, 4.0 mmol) was added. The reaction was stirred at room temperature overnight. The solvents were removed and the crude mixture dissolved in CH_2Cl_2 (50 ml), washed with water (3 × 50 ml), dried over Na_2SO_4, filtered and evaporated to dryness. The crude mixture was precipitated from hexane to give a pale brown solid (0.59 g, 91%). The compound was used without further purification. ^{1}H NMR ($CDCl_3$) 3.15–3.20 (8H, m) and 0.45 (18H, s).

Published on 18 June 2012 on http://pubs.rsc.org | doi:10.1039/C2JM32374E
Downloaded by University of Strathclyde on 23 August 2012

Published on 18 June 2012 on http://pubs.rsc.org | doi:10.1039/C2JM32374E
Downloaded by University of Strathclyde on 23 August 2012

Copolymer BDP-bis-EDOT

To a solution **6** (450 mg, 0.7 mmol) in dry toluene (50 ml) was added a solution of **4** (332 mg, 0.7 mmol) in dry toluene (25 ml). $Pd[PPh_3]_4$ catalyst (30 mg) was added and the reaction was stirred under nitrogen at 110 °C for 48 h. The reaction mixture was cooled down to room temperature and 2-bromothiophene (60 mg, 0.35 mmol) and $Pd[PPh_3]_4$ (10 mg) were added. The reaction was heated to 110 °C for 5 h and cooled down again to room temperature to add trimethyl stannylated EDOT (100 mg, 0.35 mmol) and stirred at 110 °C again overnight. The crude product was precipitated into methanol and collected by filtration. Soxhlet purification was carried out using methanol, acetone and the main fractions were extracted from CH_2Cl_2 to give a black polymer (200 mg, 44%). ^{1}H NMR ($CDCl_3$) 7.48 (2H, br), 7.28 (2H, br), 7.01 (2H, br), 6.80 (2H, br), 4.28 (8H, br), 4.06 (2H, br), 1.85 (2H, br), 1.60–1.20 (6H, br) and 0.96 (3H, br).

Copolymer BDP-bis-EDTT

To a solution of **9** (360 g, 0.5 mmol) in dry toluene (50 ml) was added a solution of **4** (233 mg, 0.5 mmol) in dry toluene (25 ml). $Pd[PPh_3]_4$ catalyst (25 mg) was added and the reaction was stirred under nitrogen at 110 °C for 48 h. The reaction mixture was cooled down to room temperature and 2-bromothiophene (50 mg, 0.25 mmol) and $Pd[PPh_3]_4$ (10 mg) were added. The reaction was heated to 110 °C for 5 h and cooled down again to room temperature to add trimethyl stannylated EDTT (125 mg, 0.35 mmol) and stirred at 110 °C again overnight. The crude product was precipitated into methanol and collected by filtration. Soxhlet purification was carried out using methanol, acetone and the main fractions were extracted from CH_2Cl_2 to give a black polymer (220 mg, 33%). ^{1}H NMR ($CDCl_3$) 7.70–7.34 (4H, br), 7.13–6.73 (4H, br), 4.07 (2H, br), 3.21(8H, br), 1.86 (2H, br), 1.63–1.26 (6H, br) and 0.96 (3H, br).

Results and discussion

Synthesis

With the aim of synthesising low band-gap polymers that bear the BODIPY core for use in OPVs,[22] bis(3,4-ethylenedioxythiophene) **(bis-EDOT)** or, its all-sulfur analogue, bis(3,4-ethylenedithiathiophene) **(bis-EDTT)** were proposed as electron donor moieties, with a BODIPY derivative as an electron acceptor. In order to solubilise the polymers and make them suitable for processing, a hexyloxy chain on the *para*-position of the benzene ring at the *meso*-position of the BODIPY was incorporated. The synthetic route (Scheme 1) was initiated by the condensation of the *para*-substituted benzaldehyde derivative with pyrrole using a high excess of pyrrole, as it also acts as solvent, in the presence of catalytic amounts of trifluoroacetic acid (TFA). Compound **2** was chlorinated on the two available *alpha*-positions of the pyrrole rings and the resultant intermediate was oxidised immediately without purification, using DDQ. This oxidation provides extension of the conjugation between the two pyrrole rings through the methylene unit. Compound **3** was deprotonated with triethylamine and reacted with $BF_3 \cdot Et_2O$ overnight at room temperature to obtain the BODIPY core **4**.

The bis-EDOT unit is a well-known moiety within organic electronics and was prepared by Ullman coupling after lithiation of EDOT and subsequent reaction with $CuCl_2$. To synthesise the second polymer, the all-sulfur analogue of bis-EDOT, bis-EDTT was also required. Following the same strategy starting from EDTT, compound **8** was synthesised in good yield. Due to the distance between the positions to be stannylated, bis-EDOT and bis-EDTT were lithiated with 2.05 equivalents of *n*-BuLi before reacting with Me_3SnCl, instead of attempting the lithiation–stannylation of the compounds in two steps. Both copolymers were obtained *via* Stille coupling of **4** (see Scheme 2), with either distannylated bis-EDOT **6** or distannylated bis-EDTT **9**, and subsequent end-capping (see Experimental). The resulting crude polymers were precipitated in methanol and purified using successive Soxhlet extractions with methanol, acetone and dichloromethane to give two black polymers, **p(BDP-bisEDOT)** and **p(BDP-bisEDTT)**. The dichloromethane fractions were characterised and used to fabricate the devices.

Electrochemical and optical properties

The HOMO and LUMO levels of both polymers were determined by cyclic voltammetry and are presented in Table 1. As previously reported,[22] the oxidation of polymers of this type results from the bis-EDOT or bis-EDTT unit, whereas the reduction results from the BODIPY core. Therefore, it is not surprising that the oxidation of the polymer is lower for the polymer containing the bis-EDOT unit as it is a stronger electron donor than the bis-EDTT analogue. The HOMO levels of the polymers were calculated from the onset of the first oxidation. The onset of the oxidation of **p(BDP-bisEDOT)** was +0.20 V and for **p(BDP-bisEDTT)** was +0.47 V, giving HOMO levels of −5.00 eV and −5.27 eV, respectively, by reference to the redox couple of ferrocene (Fig. 2). Likewise, the LUMO levels were calculated from the onset of the first reduction. As the LUMO relies on the BODIPY core, both onsets are similar (−1.15 V for **p(BDP-bisEDOT)** and −1.18 V for **p(BDP-bisEDTT)**), giving LUMO levels of −3.65 eV and −3.62 eV.

The optical properties were characterised by UV-vis spectroscopy (see Table 1). Fig. 3 shows the spectra of copolymers **p(BDP-bisEDOT)** and **p(BDP-bisEDTT)** both in dichloromethane solution and as a film drop-cast on indium tin oxide (ITO). Both copolymers show broad absorption ranges, an important parameter that favours light harvesting for OPVs. Copolymer **p(BDP-bisEDOT)** shows broad absorption from around 300 nm to 1000 nm in solution and up to 1100 nm in thin films. The thin-film of **p(BDP-bisEDOT)** shows a broad absorption peak at 821 nm that could be due to the intermolecular charge transfer (ICT) between the bis-EDOT units and the BODIPY core. The thin-film spectrum also shows a sharp peak at 426 nm and two shoulder peaks at 569 nm and 676 nm.

In the thin-film spectrum of **p(BDP-bisEDTT)** a broad absorption peak at around 669 nm is observed, which could also correspond to ICT. In **p(BDP-bisEDOT)**, the band associated to the ICT is red-shifted 152 nm compared to **p(BDP-bisEDTT)** as the bis-EDOT moiety is a stronger electron donor than bis-EDTT. **p(BDP-bisEDTT)** also shows absorption at 405 nm and 551 nm (sh). Although it is difficult to determine precisely, the optical band-gap corresponds to around 1.18 eV for

 This journal is © The Royal Society of Chemistry 2012

Published on 18 June 2012 on http://pubs.rsc.org | doi:10.1039/C2JM32374E
Downloaded by University of Strathclyde on 23 August 2012

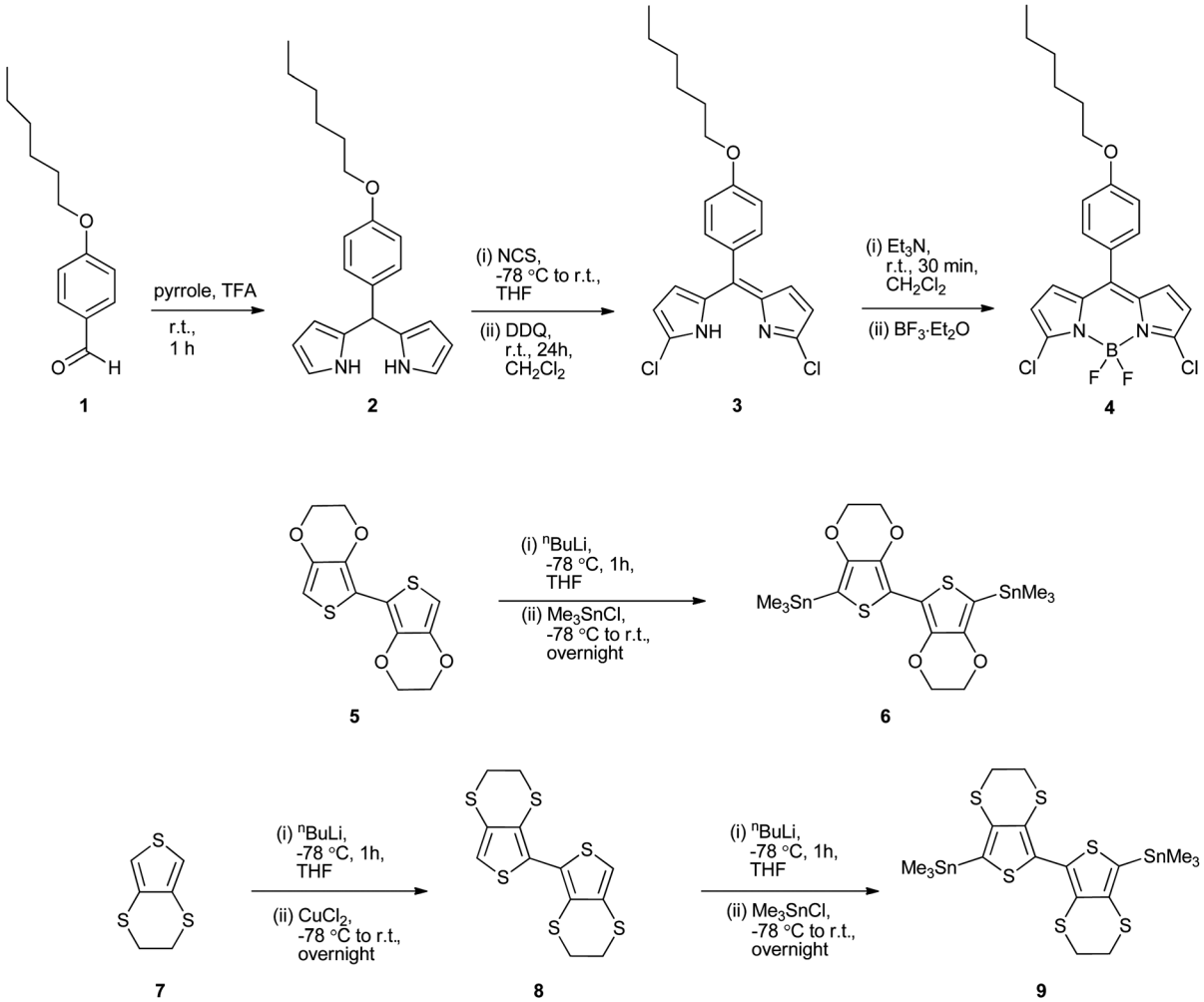

Scheme 1 Synthetic route for the synthesis of the BODIPY core, distannylated bisEDOT and bisEDTT derivatives.

p(BDP-bisEDOT) and around 1.35 eV for **p(BDP-bisEDTT)** as the onsets are around 1050 nm and 919 nm, respectively. While the EDTT units in the bis-EDTT unit are expected to be twisted, the more planar spatial configuration of bis-EDOT, due to the favourable O···S interactions between atoms of adjacent EDOT units,[24] results in a higher degree of conjugation, and hence the lower band-gap of **p(BDP-bisEDOT)**.

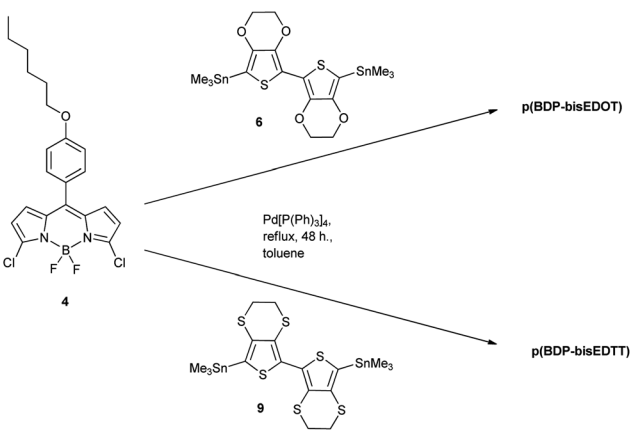

Scheme 2 Synthesis of **p(BDP-bisEDOT)** and **p(BDP-bisEDTT)**.

Device characterisation

Two types of device were fabricated, characterised and optimised. The polymer only devices demonstrated high photocurrents: 0.62 mA cm^{-2} and 1.18 mA cm^{-2} for **p(BDP-bisEDTT)** and **p(BDP-bisEDOT)**, respectively (see Fig. 4). The addition of an electron acceptor, [6,6]-phenyl-C_{71}-butyric acid methyl ester, dramatically improved performance. A donor acceptor ratio of 1 : 4 was found to be optimal for both low band-gap polymers. The power conversion efficiency increased from 0.13 to 0.95% for **p(BDP-bisEDOT)** and from 0.06% to 0.45% for **p(BDP-bisEDTT)** with photocurrents of 7.87 mA cm^{-2} and 4.42 mA cm^{-2} respectively (see Table 2). The observed decrease in V_{oc} for the polymer–fullerene devices can be attributed to the energy loss arising from electron transfer between the donor and the acceptor. Both polymer–fullerene blends demonstrate a broad spectral response (400–1100 nm). For **p(BDP-bisEDOT)**:fullerene devices an EQE of ~10, 20, 30% is observed from 400–600 nm under 0.0, −0.5, −1.0 V bias, respectively. There is

Table 1 Electrochemical, optical and molecular weight data

Cyclic voltammetry				UV-vis absorption spectra[b]			
Polymer	HOMO[a]/eV	LUMO[a]/eV	E_g/eV	$\lambda(\text{max})_{sol}$ /nm	$\lambda(\text{max})_{film}$ /nm	$E_g(\text{eV})_{film}$[c]	M_n (g mol^{-1}) (PDI)
p(BDP-bisEDOT)	−5.00	−3.65	1.35	818 (br)	821	1.18	1.7e + 05 (2.1)
p(BDP-bisEDTT)	−5.27	−3.62	1.65	648	669	1.35	3.7e + 04 (5.4)

[a] HOMO and LUMO levels were determined from the onset of the first oxidation and reduction with reference to the HOMO of ferrocene (−4.8 eV), which was used as an internal standard. [b] The UV-vis absorption spectra of the polymers were measured in dichloromethane solution and as thin films. [c] The optical band-gap was calculated from the absorption onset of films.

Published on 18 June 2012 on http://pubs.rsc.org | doi:10.1039/C2JM32374E
Downloaded by University of Strathclyde on 23 August 2012

a steady decrease in EQE from 600–900 nm. At 900 nm the EQE under 0.0, −0.5, −1.0 V bias has approximately halved. Between 900 and 1100 nm we see a sharp fall in EQE. For the **p(BDP-bisEDTT)** fullerene devices impressive EQEs are observed between 400 and 600 nm of >10, 30, 50% for 0.0, −0.5, −1.0 V bias, respectively. From 600–1100 nm we see a severe fall in EQE and it is in this region where the **p(BDP-bisEDOT)** fullerene devices outperform the **p(BDP-bisEDTT)** fullerene devices. The large EQE in the 400–700 nm region can be attributed to the [6,6]-phenyl-C_{71}-butyric acid methyl ester absorption and its ability to effectively dissociate the exciton allowing them to contribute to photocurrent (see Fig. 5).

Fig. 6 shows tapping mode height images of atomic force microscopy (AFM). The image shows the presence of small bead-like structures of **p(BDP-bisEDOT)** spin-coated on ITO/PEDOT substrates. The root mean square (rms) roughness was calculated as 42 nm by taking into account a 10 μm × 10 μm scan area that would reflect the actual device under test. While the surface roughness on smoother areas is around 20 nm, the small bead-like structures tend to aggregate and form slightly bigger domains with heights of up to 100 nm. This mixture of aggregate and non-aggregate regions provides a higher average rms roughness of ~42 nm. Tapping mode AFM images recorded on glass substrates (available in the ESI†) exhibit lower rms surface roughness of ~22 nm. Smooth bead-like structures are observed on both substrates (on glass and on ITO/PEDOT/**p(BDP-bisEDOT)**). However, there are fewer aggregated domains consisting of bigger structures with height of ~100 nm in the **p(BDP-bisEDOT)** coated on glass than for ITO/PEDOT/**p(BDP-bisEDOT)**. This type of aggregation caused by the wettability of solutions of **p(BDP-bisEDOT)** on different substrates can be improved by optimising thin film fabrication protocols.

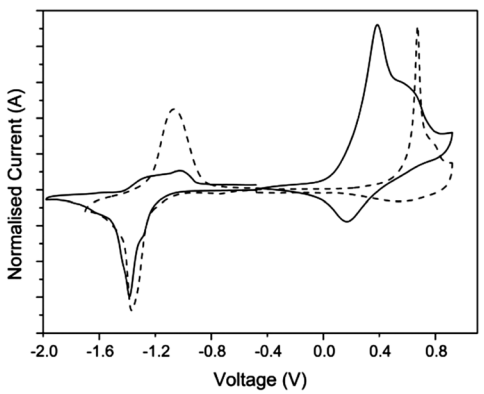

Fig. 2 Cyclic voltammetry of **p(BDP-bisEDOT)** (solid line) and **p(BDP-bisEDTT)** (dashed line). Each film was deposited from a solution of the polymer in dichloromethane on a glassy carbon electrode and experiments were carried out in acetonitrile in the presence of Bu_4NPF_6 (0.1 M). A Ag wire reference electrode and a Pt counter electrode were used. All the values are quoted *versus* the redox potential of the ferrocene/ferrocenium couple.

Time of flight measurements

To understand more completely the behaviour of **p(BDP-bisEDOT)** in solar cell devices without a separate acceptor component, both electron and hole mobility were studied by time of flight (TOF). Fig. S5a† shows the **p(BDP-bisEDOT)** linear hole photocurrent transient at an electric field of

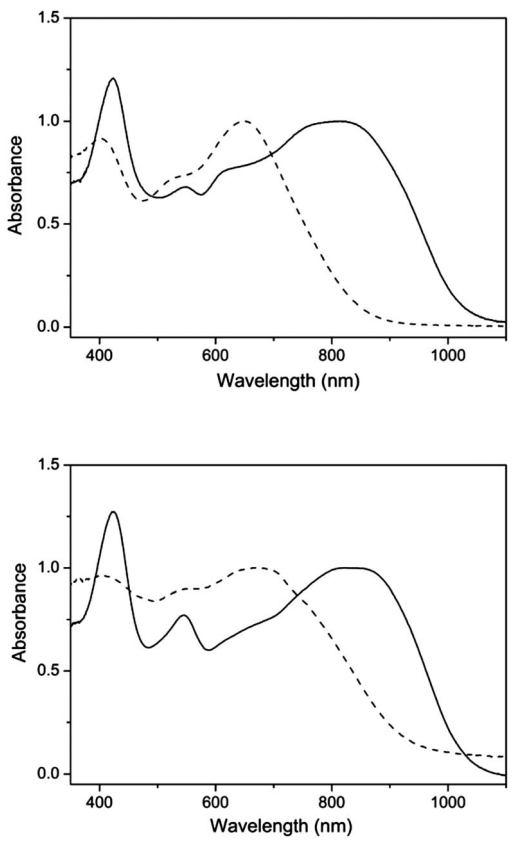

Fig. 3 Normalised optical absorption spectra of **p(BDP-bisEDOT)** (solid line) and **p(BDP-bisEDTT)** (dashed line) in dichloromethane (top) and in the solid state (bottom).

This journal is © The Royal Society of Chemistry 2012

Published on 18 June 2012 on http://pubs.rsc.org | doi:10.1039/C2JM32374E
Downloaded by University of Strathclyde on 23 August 2012

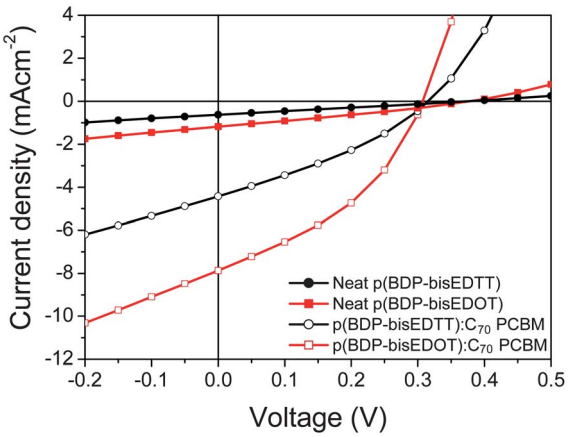

Fig. 4 *J–V* characteristics for polymer and polymer–fullerene devices under 100 mW cm^{-2} illumination with standard AM 1.5G source.

1.8×10^5 V cm^{-1}. The photocurrent transient shows that the transport is highly dispersive since the linear plot has an exponential like decay instead of a definitive cusp, a plateau and clearly defined knee. However, by plotting the photocurrent transient in a log–log scale, a change in the slope was visible. The transit time was determined at each electric field by fitting straight lines before and after the knee as shown in Fig. S5b†. For the above applied electric field the transit time was 39 μs, which corresponds to a mobility value of 1.5×10^{-5} cm^2 V^{-1} s^{-1}. Fig. S6a† shows the **p(BDP-bisEDOT)** linear electron photocurrent transient at about 1.8×10^5 V cm^{-1}. Again the electron photocurrent transient is highly dispersive, thus a log–log scale plot was necessary to observe a change in the slope of the photocurrent transient (Fig. S6b†). For the above applied electric field the transit time was 7 μs, which corresponds to a mobility value of 7.7×10^{-5} cm^2 V^{-1} s^{-1}.

TOF mobility measurements were performed in a wide range of electric fields in order to investigate the field dependence of the mobility. Fig. 7 shows both electron and hole mobility as a function of the square root of the electric field. The most important result is that **p(BDP-bisEDOT)** is an ambipolar charge transport carrier material. In fact both electron and hole mobility values are of the same order of magnitude. Usually for a p-type (n-type) material, electron mobility is orders of magnitude lower than hole mobility, or *vice versa*. However, we can clearly see from Fig. 7 that electron mobility values are approximately three times higher than hole mobility, indicative of ambipolar behaviour.

Furthermore, Fig. 7 demonstrates that both carriers show a similar field dependence. It can be clearly seen that at low fields ($E < 3 \times 10^5$ V cm^{-1} [$E^{1/2} < 600$ V cm^{-1}]) mobility is nearly field independent and its value turned out to be in the range of 2.5×10^{-5} cm^2 V^{-1} s^{-1} and 7.5×10^{-5} cm^2 V^{-1} s^{-1}, for the holes and the electrons respectively. As the electric field increases further

Table 2 Photovoltaic devices

Active layer	J_{sc}/mA cm^{-2}	V_{oc}/V	FF [%]	PCE [%]
p(BDP-bisEDOT)	1.18	0.38	29	0.13
p(BDP-bisEDTT)	0.62	0.37	26	0.06
p(BDP-bisEDOT):[70]PCBM[a]	7.87	0.31	39	0.95
p(BDP-bisEDTT):[70]PCBM[a]	4.42	0.32	32	0.45

[a] Ratio: polymer:[70]PCBM (1 : 4).

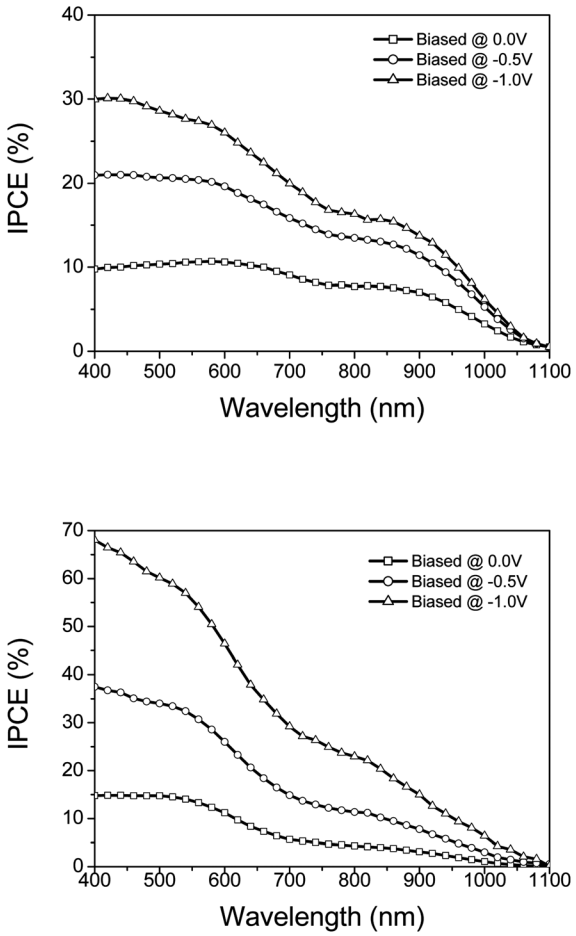

Fig. 5 Incident photon to electron conversion efficiency (IPCE) for polymer–fullerene devices with and without bias **p(BDP-bisEDOT)** (top) and **p(BDP-bisEDTT)** (bottom).

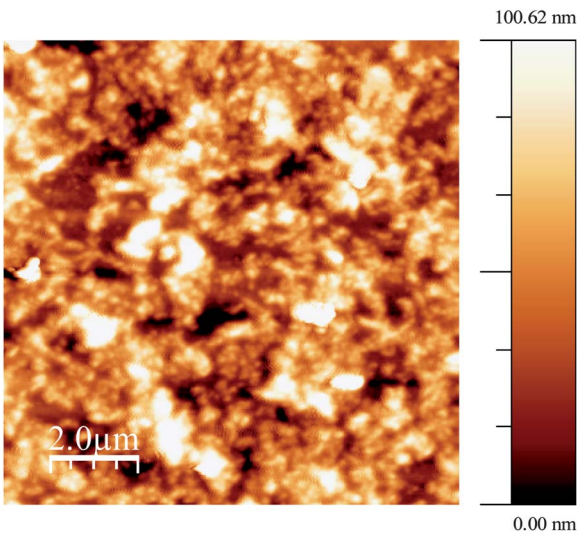

Fig. 6 Tapping mode AFM height images of **p(BDP-bisEDOT)** on ITO/PEDOT substrate.

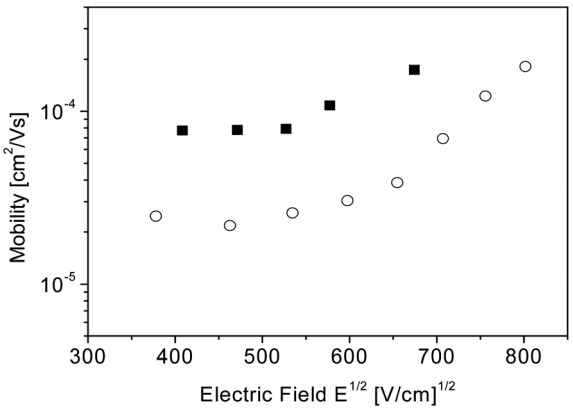

Fig. 7 Electron (squared dots) and hole (circular dots) mobilities of **p(BDP-bisEDOT)** against the electric field.

a classic Poole–Frenkel like mobility dependence is shown. Mobility increases nearly an order of magnitude from 3×10^{-5} $cm^2\ V^{-1}\ s^{-1}$ up to 2×10^{-4} $cm^2\ V^{-1}\ s^{-1}$ for the holes and from 7×10^{-5} $cm^2\ V^{-1}\ s^{-1}$ up to 3.2×10^{-4} $cm^2\ V^{-1}\ s^{-1}$ for the electrons as the field increases from 3.5×10^5 V cm^{-1} to 6.5×10^5 V cm^{-1}.

Conclusion

Two new low band-gap copolymers based on a BODIPY core and the well-known bis-EDOT and bis-EDTT units have been synthesised *via* Stille coupling. The polymers have an optical band-gap of 1.18 and 1.35 eV for **p(BDP-bisEDOT)** and **p(BDP-bisEDTT)**, respectively, and demonstrate respectable short circuit current densities for pristine devices implying ambipolar charge transport. TOF measurements on **p(BDP-bisEDTT)** show electron and hole mobilities to be of the same order of magnitude confirming ambipolar charge transport. When blended with a soluble fullerene a power conversion efficiency of 0.95% and 0.45% is observed for **p(BDP-bisEDOT)** and **p(BDP-bisEDTT)**, respectively. The broad spectral response demonstrated by these polymer–fullerene devices makes these materials possible candidates for future broadband light sensing and harvesting applications.

References

1 C. W. Tang, *Appl. Phys. Lett.*, 1986, **48**, 183.
2 R. Kroon, M. Lenes, J. C. Hummelen, P. W. M. Blom and B. de Boer, *Polym. Rev.*, 2008, **48**, 531; B. C. Thompson and J. M. J. Fréchet, *Angew. Chem., Int. Ed.*, 2008, **47**, 58; F. G. Brunetti, R. Kumar and F. Wudl, *J. Mater. Chem.*, 2010, **20**, 2934; J. L. Delgado, P. Bouit, S. Filippone, M. A. Herranz and N. Martín, *Chem. Commun.*, 2010, **46**, 4853; G. Dennler, M. C. Scharber and C. J. Brabec, *Adv. Mater.*, 2009, **21**, 1323.
3 G. Yu, J. Gao, J. C. Hummelen, F. Wudl and A. J. Heeger, *Science*, 1995, **270**, 1789–1791.
4 J. J. M. Halls, C. A. Walsh, N. C. Greenhan, E. A. Marseglia, R. H. Friend, S. C. Moratti and A. B. Holmes, *Nature*, 1995, **376**, 498.
5 H. Chen, J. Hou, S. Zhang, Y. Liang, G. Yang, Y. Yang, L. Yu, Y. Wu and G. Li, *Nat. Photonics*, 2009, **3**, 649; S. H. Park, A. Roy, S. Beaupré, S. Cho, N. Coates, J. Moon, D. Moses, M. Leclerc, K. Lee and A. J. Heeger, *Nat. Photonics*, 2009, **3**, 297; J. Hou, H. Chen, S. Zhang, R. I. Chen, Y. Yang, Y. Wu and G. Li, *J. Am. Chem. Soc.*, 2009, **131**, 15586; C. Piliego, T. W. Holcombe, J. D. Douglas, C. H. Woo, P. M. Beaujuge and J. M. J. Frechet, *J. Am. Chem. Soc.*, 2010, **132**, 7595; M. M. Wang, X. Hu, P. Liu, W. Li, X. Gong, F. Huang and Y. Cao, *J. Am. Chem. Soc.*, 2011, **133**, 9638; C. M. Amb, S. Chen, K. R. Graham, J. Subbiah, C. E. Small, F. So and J. R. Reynolds, *J. Am. Chem. Soc.*, 2011, **133**, 10062; E. Wang, Z. Ma, Z. Zhang, K. Vandewal, P. Henriksson, O. Inganas, F. Zhang and M. R. Andersson, *J. Am. Chem. Soc.*, 2011, **133**, 14244.
6 J. Nelson, *Mater. Today*, 2011, **14**, 462.
7 N. S. Sariciftci, L. Simliowitz, F. Wudl and A. J. Heeger, *Science*, 1992, **258**, 1474.
8 P. E. Shaw, A. Ruseckas and I. D. W. Samuel, *Adv. Mater.*, 2008, **20**, 3516.
9 A. Ruseckas, P. E. Shaw and I. D. W. Samuel, *Dalton Trans.*, 2009, 10040.
10 D. E. Markov, C. Tanase, P. W. M. Blom and J. Wildeman, *Phys. Rev. B: Condens. Matter Mater. Phys.*, 2005, **72**, 045217; D. E. Markov, E. Amsterdam, P. W. M. Blom, A. B. Sieval and J. C. Hummelen, *J. Phys. Chem. A*, 2005, **109**, 5266; J. M. C. R. Nunzi, *Physique*, 2002, **3**, 523.
11 G. Li, V. Shrotriya, J. Huang, Y. Yao, T. Moriarty, K. Emery and Y. Yang, *Nat. Mater.*, 2005, **4**, 864; W. Ma, C. Xang, X. Gong, K. Lee and A. J. Heeger, *Adv. Funct. Mater.*, 2005, **15**, 1617.
12 J. Roncali, *Chem. Rev.*, 1997, **97**, 173.
13 H. Zhou, L. Yang and W. You, *Macromolecules*, 2012, **2**, 607.
14 C. J. Brabec, C. Winder, N. S. Sariciftci, J. C. Hummelen, A. Dhanabalan, P. A. van Hal and R. A. J. Janssen, *Adv. Funct. Mater.*, 2002, **12**, 709.
15 H. A. Becerril, N. Miyaki, M. L. Tang, R. Mondal, Y. Sun, A. C. Mayer, J. E. Parmer, M. D. McGehee and Z. Bao, *J. Mater. Chem.*, 2009, **19**, 591.
16 J. C. Bijleveld, A. P. Zoombelt, S. G. J. Mathijssen, M. M. Wienk, M. Turbiez, D. M. de Leeuw and R. A. J. Janssen, *J. Am. Chem. Soc.*, 2009, **131**, 16616; J. C. Bijleveld, V. S. Gevaerts, D. Di Nuzzo, M. Turbiez, S. G. J. Mathijssen, D. M. de Leeuw, M. M. Wienk and R. A. J. Janssen, *Adv. Mater.*, 2010, **22**, E242–E246.
17 M. C. Scharber, D. Mühlbacher, M. Koppe, P. Denk, C. Waldauf, A. J. Heeger and C. J. Brabec, *Adv. Mater.*, 2006, **18**, 789.
18 A. Loudet and K. Burgess, *Chem. Rev.*, 2007, **107**, 4891; G. Ulrich, R. Ziessel and A. Harriman, *New J. Chem.*, 2007, **31**, 496; G. Ulrich, R. Ziessel and A. Harriman, *Angew. Chem., Int. Ed.*, 2008, **47**, 1184.
19 Q. D. Zheng, G. X. Xu and P. N. Prasad, *Chem.–Eur. J.*, 2008, **14**, 5812; Y. Ikawa, S. Moriyama and H. Furuta, *Anal. Biochem.*, 2008, **378**, 166; M. A. H. Alamiry, A. C. Benniston, G. Copley, K. J. Elliott, A. Harriman, B. Stewart and Y. G Zhi, *Chem. Mater.*, 2008, **20**, 4024; O. Garcia, L. Garrido, R. Sastre, A. Costela and I. Garcia-Moreno, *Adv. Funct. Mater.*, 2008, **18**, 2017; A. Costela, I. Garcia-Moreno, M. Pintado-Sierra, M. Amat-Guerri, M. Liras, R. Sastre, F. L. Arbeloa, J. B. Prieto and I. L. Arbeloa, *J. Photochem. Photobiol., A*, 2008, **198**, 192; S. Mula, A. K. Ray, M. Banerjee, T. Chaudhuri, K. Dasgupta and S. Chattopadhyay, *J. Org. Chem.*, 2008, **73**, 2146; S. Erten-Ela, M. D. Yilmaz, B. Icli, B. Y. Dede., S. Icli and E. U. Akkaya, *Org. Lett.*, 2008, **10**, 3299; L. Bonardi, H. Kanaan, F. Camerel, P. Jolinat, P. Retailleau and R. Ziessel, *Adv. Funct. Mater.*, 2008, **18**, 401; M. M. Sartin, F. Camerel, A. J. Ziessel and J. Bard, *J. Phys. Chem. C*, 2008, **112**, 10833.
20 M. D. Yilmaz, O. A. Bozdemir and E. U. Akkaya, *Org. Lett.*, 2006, **8**, 2871.
21 R. Ziessel, C. Goze, G. Ulrich, M. Cesario, P. Retailleau, A. Harriman and J. P. Rostron, *Chem.–Eur. J.*, 2005, **11**, 7366–7378.
22 J. C. Forgie, P. J. Skabara, I. Stibor, F. Vilela and Z. Vobecka, *Chem. Mater.*, 2009, **21**, 1784.
23 A. Cihaner and F. Algi, *Electrochim. Acta*, 2008, **54**, 786; A. Cihaner and F. Algi, *React. Funct. Polym.*, 2009, **69**, 62; F. Algi and A. Cihaner, *Org. Electron.*, 2009, **10**, 453.
24 H. J. Spencer, P. J. Skabara, M. Giles, I. McCulloch, S. J. Coles and M. B. Hursthouse, *J. Mater. Chem.*, 2005, **15**, 4783.

Published on 18 June 2012 on http://pubs.rsc.org | doi:10.1039/C2JM32374E
Downloaded by University of Strathclyde on 23 August 2012

This journal is © The Royal Society of Chemistry 2012